

Design of a Low Respiratory Resistance Mask for COVID-19

YANG Pufan^{a,b} (杨朴凡), HUANG Hongxin^{a,b} (黄洪鑫) WEI Siji^a (卫思霁),
YAO Yuan^a (姚远), ZHANG Zhinan^{a,b*} (张执南)
(a. School of Mechanical and Engineering; b. iDesignLab, Student Innovation Center,
Shanghai Jiao Tong University, Shanghai 200240, China)

© Shanghai Jiao Tong University 2022

Abstract: Observational evidence suggests that mask-wearing mitigates transmission of COVID-19; at the same time high respiratory resistance leads to an unwillingness to wear masks. This paper proposed a respiratory drive structure to reduce the air resistance of a mask. This structure provides different shapes during expiration and inspiration while focusing on filtering dust, bacteria, or viruses. Meanwhile, the assembled system on the mask can be disassembled and replaced. Then porous media simulation is used to verify the model effect. Experimental results of a new mask show that the ventilation resistance is reduced by 20%, and the bacterial filtration efficiency meets the requirements of YY 0469—2011.

Key words: mask, conceptual structure, respiratory resistance, bacterial filtration efficiency

CLC number: TH 122 **Document code:** A

0 Introduction

As the Corona Virus Disease 2019 (COVID-19) can be transmitted from person to person via respiratory droplets, prevention and control are more difficult^[1]. Nowadays, people should pay more attention to personal protection, in which masks play an essential role^[2-4].

In such a “worldwide fight against the epidemic of COVID-19”, masks are the necessary prevention equipment used by billions of people, common but not straightforward^[5]. In the case of insufficient supply of masks, researchers from various countries have tried many alternatives to masks, but the effect is unsatisfactory^[6-8]. The mask design requires precision, reliability, comfort, ergonomics, and life science-related standards^[9]. Due to different use environments and main protection objects, masks are divided into different types^[10]. According to the degree of dependence on the external environment, personal protective equipment (PPE) can be divided into atmosphere-supplying respiratory protective equipment and air-purifying respiratory protective equipment. In this paper, the mask belongs to the second one. There are two types of masks, which are self-inspiration masks, and powered masks. A self-inspiration mask means the wearer over-

comes the resistance of parts by breathing instead of relying on other power sources, such as electric fans^[11].

The existing masks have many problems that need to be solved, such as large respiratory resistance and uncomfortable feeling. Scholars from all around the world study how to reduce respiratory resistance when wearing masks. Ding and Jia^[12] analyzed 21 popular types of masks and found out that although masks with a valve have a lower expiration resistance, the occupation of an area on the masks leads to increased inspiration resistance. If the valve’s design, material, and manufacturing process are inadequate, respiratory resistance will increase. Shi and Gao^[13] summarized and analyzed the patents related to nanofiber membranes and pointed out that applying nanofiber membranes in making masks has three advantages: higher barrier efficiency, longer service life, and better air permeability. However, the high costs factor disturbs the widespread promotion of this application. Liu et al.^[14] studied the relationship between respiratory resistance, fiber network structure, and aerosol flow rate. They found out that the respiratory resistance increases linearly with the increase of the aerosol flow rate and increases with the fiber network’s average pore diameter. Tian et al.^[15] pointed out that after wearing the N95 mask, the air exchange volume is reduced by an average of 37%, causing a part of carbon dioxide to be inspired when inspiration again. They also found out that the cup-type mask has a lower breathing resistance rate than the folding mask. The new breathing pattern is similar to the standard deep breathing method, which

Received: 2020-11-13 **Accepted:** 2021-03-29

Foundation item: the Project of Establishing a Base for Training Interdisciplinary Innovative Talents with Practice at Shanghai Jiao Tong University

***E-mail:** zhinanz@sjtu.edu.cn

can be referred to while developing new masks. Yao et al.^[16] studied the mask’s structural characteristics on mask’s respiratory resistance and found that the cup-type mask has a lower change rate of breathing resistance than the folding mask. The planar mask has a more comfortable wearing sensation; however, it has lowered the protection level. Therefore, it is necessary to consider comfort sensation and protection level when choosing a mask .

The traditional two-way filtration without the valve masks has lasted for a long time. Nowadays valve masks with one-way filtration function are being used. In the future, the “new generation” of valve masks should realize two-way filtration and develop in the direction of ultra-thin, ultra-light, low resistance, high efficiency, and two-way ultra-precision filtration. Therefore, the purpose of this paper is to explore a kind of new mask with low resistance.

In general, three methods can be used to achieve smoothness during breathing by using the mask: increasing the number of valves, changing the hardness and thickness of the diaphragm, and structural improvement. Zhang^[17] designed a mask structure with two breathing valves. Even this structure is simple, the filtration efficiency of PM_{2.5} can reach 95%. Gu et al.^[18] improved the mask diaphragm’s hardness and thickness, making this structure suitable for diving. Nevertheless, these designs only consider protecting the wearer, and they ignore the potential danger of wear. Zhu and Niu^[19-20] improved the valve structure by adding the extra component to balance pressure. However, more elements can cause unwanted total equipment conflict. The most important contradiction is not able to decrease the respiratory resistance while improving the comfort together.

People have the requirements of protection, safety, and comfort for the daily use of masks. Among them, comfort refers to whether the face pressure is sensible or not. Moreover, it does not affect the face’s activities. The most crucial point is the smoothness during breathing. Therefore, this paper explores the conceptual design of a low-resistance mask and evaluates its design effect. The paper is divided into four parts: analysis of the mask’s functional structure, the conceptual design,

the simulation and evaluation of the design model, and prototyping and verification.

1 Functional Analysis

The general medical surgical mask has three layers. The outer layer is a hydrophobic nonwoven fabric that prevents the invasion of external water and blood. The intermediate layer is a melt jet cloth treated by electret, which mainly absorbs bacteria and viruses. The inner layer is another hydrophilic nonwoven fabric, which absorbs the human body’s moisture to ensure comfort. Although this mask is widely used nowadays, it still has an uncomfortable feeling during wearing due to respiratory resistance.

Environment-based design (EBD) and functional structure analysis methods are used to design the mask^[21-22]. The environmental factors are comprehensively considered, and then the functional structure classification analysis is carried out. As shown in Fig. 1, the primary users of the mask designed in this paper are asymptomatic or potentially susceptible to infection. Under the driving of respiration, the respirator ensures users’ safety and comfort. Among them, breathing can be further subdivided into the expiration process and inspiratory process, depending on different filtering targets. On a daily basis, people wear masks to protect themselves from dust, small particles, viruses, and bacteria during respiration. However, masks are also protecting other people from the virus-carrying mask wearers. In this process, there is a difference between the primary filter objects when expiration and inspiration. These differences provide the possibility to improve the resistance of the mask.

The filtration principle can be divided into inertial impaction, interception, diffusion, and electrostatic attraction. When passing through the filter layer, large particles are affected by gravity and other factors. It is mechanically collided with the filter materials and finally intercepted, while small particles are randomly adsorbed. The main power of filtration for bacteria and viruses is the attraction of the electrostatic field. For water vapor, the adsorption filtration mainly depends on the hydrophilicity of the material.

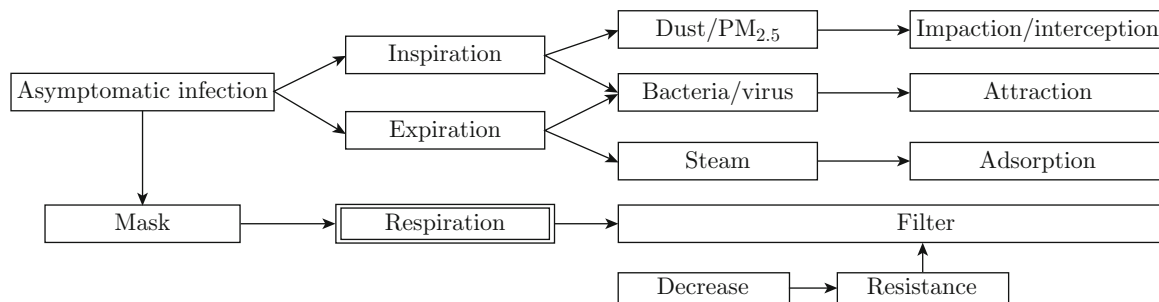


Fig. 1 Functional analysis

The process of mask filtration is further analyzed, as shown in Figs. 2 and 3. Generally, for various properties to be filtered, layered and batch filtration methods will be adopted. The filtration of dust and particulate matter does not exist in the process of expiration and inspiration. Moreover, it often leads to the blockage of mask microstructure, which increases respiratory resistance. Therefore, it is necessary to separate the filter layer for dust and microparticles.

Two fundamental issues have been found through the

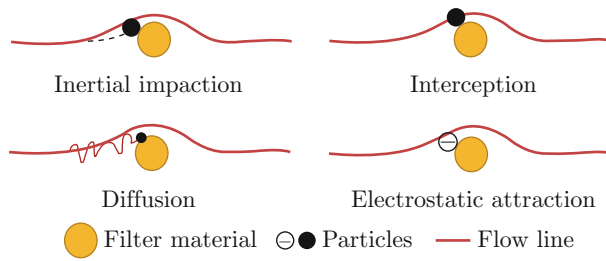


Fig. 2 Filtration mechanisms

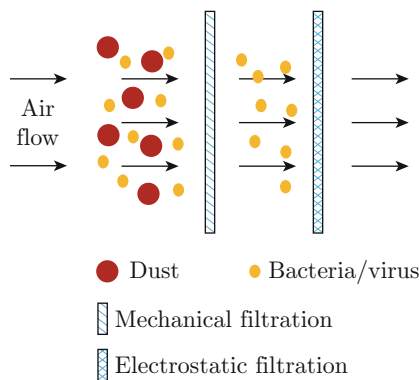


Fig. 3 Filtration progress

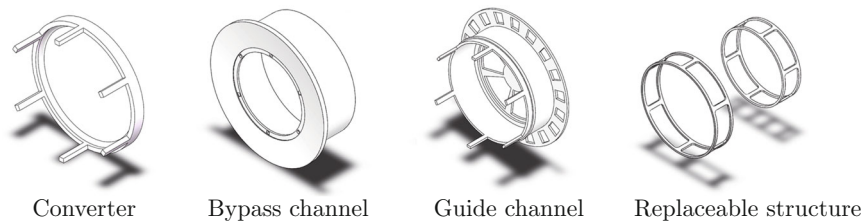


Fig. 4 Key structural units

2.1.1 Natural Drive Converter by Breathing

The converter is the fundamental unit, which is located in the center of the device. It can move back and forth in the set channel with the pressure difference generated by expiration. Therefore, it can realize the change of filtration effect during inspiration and expiration. The converter can simulate normal mask breathing's slight amplitude vibration to make the converter

analysis of the filtration principle. First, filtration efficiency and respiratory resistance have a contradiction. The improvement of filtration efficiency generally depends on the refinement of the filter material mesh. Moreover, the mesh's refinement will inevitably lead to a decrease of the interface through the respiratory process, which will lead to an increase of resistance. Second, the emphasis on expiratory and inspiratory filtration is different. The filtration of external dust and particles should be considered when inspiration, and the water vapor should be considered when expiration.

Meanwhile, mask tightness refers to the degree of tightness between the mask periphery and the specific user's face, which is an essential item. The mask determines filtration efficiency. However, if the respirator does not fit the user's face tightly, harmful substances in the air will enter the mask from the leakage gap and enter the respiratory tract. Therefore, based on the existing one-way valve mask structure, retaining the differential breathing structure design and increasing the common safety guarantee mechanism are the key points of mechanical structure design.

2 Conceptual Design

2.1 Preliminary Conceptual Design

According to the principal analysis, the proposed new design mask's core structure needs at least two layers, one layer to filter dust and microparticles, while the other layer to filter virus and bacteria. To ensure the comfort of wearing the mask, it is also necessary to increase the inner hydrophilic layer. The filter layer is sufficient for dust particles during inspiration and should leave the flow channel when expiratory. Therefore, the preliminary conceptual design is completed based on the idea of a one-way valve mask. Figure 4 shows the vital structural units.

move fluently, while the weight should be maintained as light as possible. Therefore, the converter's thickness is designed as thin as possible, and six slender bars are designed to control the amplitude. Openings in the sidewalls also provide airflow channels.

2.1.2 Uniform Flow Structure to Reduce Resistance

The guide channel is used to fix the stroke of the converter. At the same time, the airflow path is

determined. Both of them restrict the converter’s vibration amplitude, guide the air to complete the uniform flow around the cylinder, and reduce the additional resistance symmetrically. This structure contains two parts: the bypass channel and the guide channel. The inner part is the guide channel which is close to the converter. The inside step structure is designed to limit the travel of the converter. At the same time, the outside step structure is designed to fix the replaceable structure.

Moreover, a fan-type structure is added at the guide channel’s outer side to prevent large objects from entering to protect the internal structure. The outer part acts as the bypass channel, which is also the whole structure’s shell. In the bypass channel, the side near the human’s face is designed as a curve surface. Therefore, it can fit the human’s face and make a comfortable feeling during usage.

2.1.3 Element Structure of Replaceable Filter

The inner and outer filter layers are arranged on two carriers, respectively. The inner filter layer cooperates

with the converter to enter the flow channel when inspiration to realize bilateral filtration. During expiration, it leaves the flow channel and retains unilateral filtration to reduce resistance. The outer filter layer cooperates with the guide channel to maintain continuous single-layer filtration. The central filter element is designed as a replaceable structure, which is assembled at the overall structure’s key filtering points to increase the mask’s usage duration. The two structures are almost identical, only differing in size.

2.2 Overall Mechanical Structure

The whole structure consists of six parts; two of them are replaceable. Figure 5 shows the exploded view of total parts, the main view, and the left view. These six parts include a fixed base, a bypass channel, two filter fixtures, a converter, and a guide channel. These parts are combined with common connection types to simplify the manufacturing and assemble process.

The converter realizes reciprocating motion under natural breathing pressure difference. The mask’s structure during inspiration is shown in Fig. 6(a). The

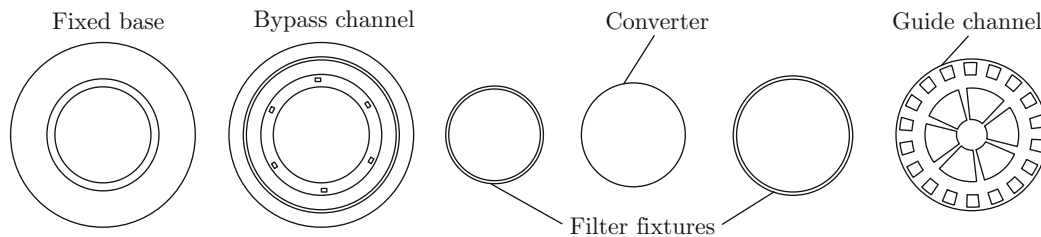


Fig. 5 Exploded view of filter structure

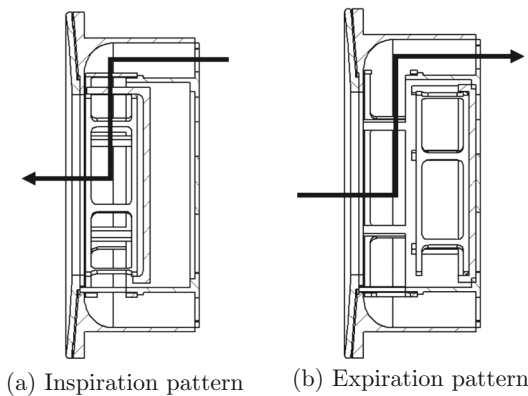


Fig. 6 Cutaway view of filter structure

left side is close to the face, while the right side is set on the outside of the mask. The external pressure is greater than the inner pressure, and the pressure difference drives the converter to move towards the fixed base. Moreover, the two-filter material clamps the overlap areas, realizing double filtration and effectively protecting the virus infection. Similarly, the mask’s structure during expiration is shown in Fig. 6(b). The external pressure is less than the inner pressure. The

pressure difference drives the converter to move to the side far away from the fixed base. The internal filter material clamp leaves the gas channel to reduce the expiratory resistance.

2.3 Selection of Materials and Parameters

2.3.1 Materials Selection

There are mature filter materials to be selected. The materials used in the medical-surgical masks’ three-layer structure can be assembled on the replaceable fixed parts of filter materials, respectively. In the material selection of the whole structure, we need to consider the strength, density, biocompatibility, and other factors and consider the material’s processing difficulty. Finally, the photosensitive resin used for the 3D printing appliance is selected as the structural material. The photosensitive resin has a density of 1.15 g/cm³, tensile strength of 50 MPa, and bending strength of 65 MPa, and is biocompatible.

2.3.2 Parameters Selection

The designed structure is referred to the size of the existing one-way valve mask to ensure that it does not affect the normal movement during the wearing. The overall diameter is 40–60 mm, in which the gas

channel diameter is about 30 mm, and the thickness is usually controlled at 5 mm. Based on this, considering the proportion of the cross-sectional area of the flow channel in the whole mask’s filtering area, the inner diameter of the gas channel is 30 mm. The outer diameter of the overall structure is 60 mm. Under these parameter conditions, the channel’s cross-sectional area approximately has a similar dimension to ensure the gas passage’s uniformity. Therefore, the dimensions of the parts, including the gas channel, are further calculated.

3 Simulation of System

3.1 Target

In this study, a kind of mask with bidirectional filtration and low respiratory resistance was designed. The simulation is carried out to verify the results of the design. The structure conversion process in two states of breathing and the distribution of airflow velocity and respiratory resistance direction and size are simulated. The designed mask structure’s scientificity and reliability are demonstrated and optimized according to the simulation results.

3.2 Parameter Setting

ANSYS 19.2 is used for simulation. This simulation uses 3D mesh to divide the fluid domain to ensure the accuracy of fluid simulation. The following assumptions are made for the simulation process:

- (1) The airflow velocity of each time breath is equal.
- (2) The structure joint is completely sealed without air leakage.
- (3) The resistance of the converter in the channel movement can be ignored.
- (4) The filter material deformation is not considered in the process.
- (5) The valve structure is rigid and does not produce plastic deformation.

First, a fluid domain includes two main parts, which are air and filters. The assembly is imported into ANSYS software for meshing. Because the thickness of the filter layer is only 2 mm, the square grid size is set to 0.2 mm to ensure that the fluid characteristics of the porous media layer can be accurately simulated.

After that, the medium parameter is chosen. The fluid area conations airflow and filter. Usually, the filter layer is treated as a porous medium. The obtained medium parameters are shown in Table 1. Among them, the air medium’s density and viscosity parameters at 25 °C are selected. The parameters of porous media are determined by analyzing the filter layer of the standard mask.

The state of airflow is not consistent during expiration and inspiration. The tidal volume and airflow of ordinary people are shown in Table 2. However, the airflow during the test is higher in the corresponding standards. Therefore, the simulation analysis is car-

Table 1 Medium parameter

Medium	Parameter	Value
Air	Density/(kg·m ⁻³)	1.225
	Viscosity/(kg·m ⁻¹)	1.789 4×10 ⁻⁵
Porous medium	Inertia resistance coefficient/m ⁻¹	4.439
	Viscous drag coefficient/m ⁻²	2.717 7×10 ⁶

Table 2 Simulation parameter

	Parameter	Value
Normal people	Airflow velocity rate/(L·min ⁻¹)	6—10
	Respiratory rate/(min ⁻¹)	12—20
	Tidal volume/mL	500
Standard	Airflow velocity rate/(L·min ⁻¹)	85

ried out for different airflow velocity rates and different expiratory (inspiratory) states.

In this simulation, the realizable *k-ε* model is used. The inlet type is chosen velocity-inlet, and the outlet type is chosen pressure-outlet. Moreover, the energy is considered and used to judge whether it converges or not. When the energy is less than 10⁻⁶ or stable, the simulation results are considered to converge.

3.3 Analysis

The simulation includes the state of different air velocities. The results of the simulation show the effect of airflow velocity on resistance.

3.3.1 Influence of Respiratory State on Resistance

Figure 7 shows four images that correspond to different fluid domain states and breathing states, respectively. In Figs. 7(b) and 7(c), the converter is at the far end. When inspiration, the airflow enters through the radial channel, where the internal air velocity gets small. When the pressure difference reaches 10 Pa, it can push the converter to the near end. Similarly, during expiration, the transducer is pushed to the far end by the pressure difference.

3.3.2 Influence of Air Velocity on Resistance

Setting the fixed value for the other parameters, the inspiratory velocity rate is set into 6 L/min, 60 L/min, and 600 L/min, separately. The corresponding pressure and velocity distribution are shown in Figs. 8 and 9. The daily respiratory rate is about 6 L/min. In some exceptional cases, such as sneezing, the airflow velocity will change suddenly, with a maximum of 600 L/min.

In the suction state, the intermediate converter is close to the base, and the relative space of the intermediate fluid domain becomes small. According to the pressure distribution, the average pressure of the outer channel is higher than that of the central part, so the two filters set in the radial direction have enough pressure to drive. From the velocity distribution, it can be

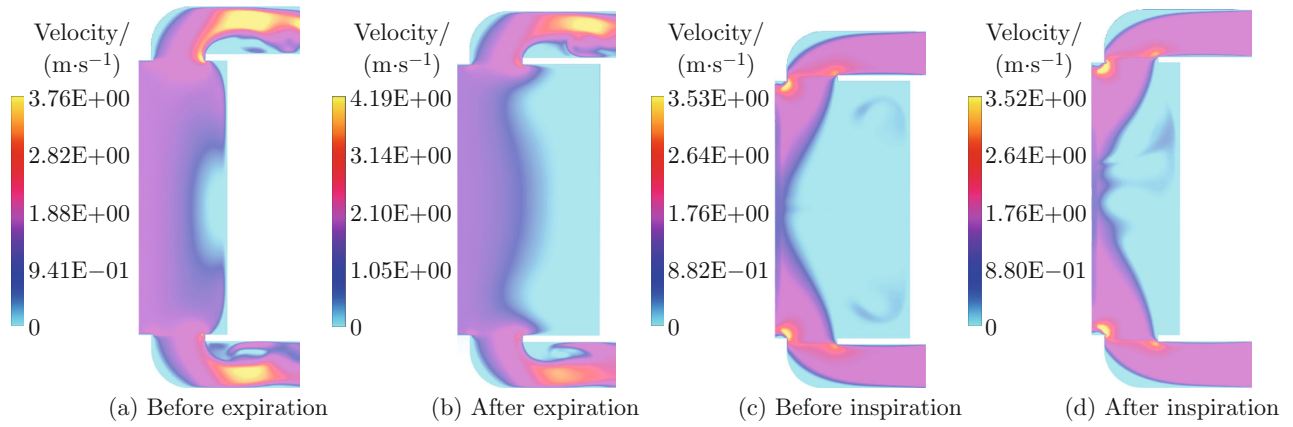


Fig. 7 Velocity distribution at different respiratory states

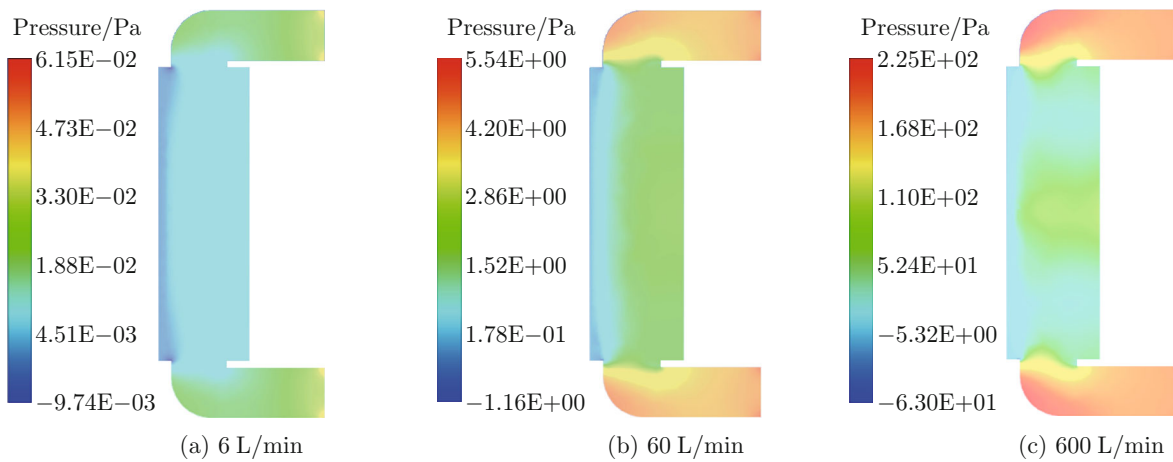


Fig. 8 Pressure distribution in inspiratory state

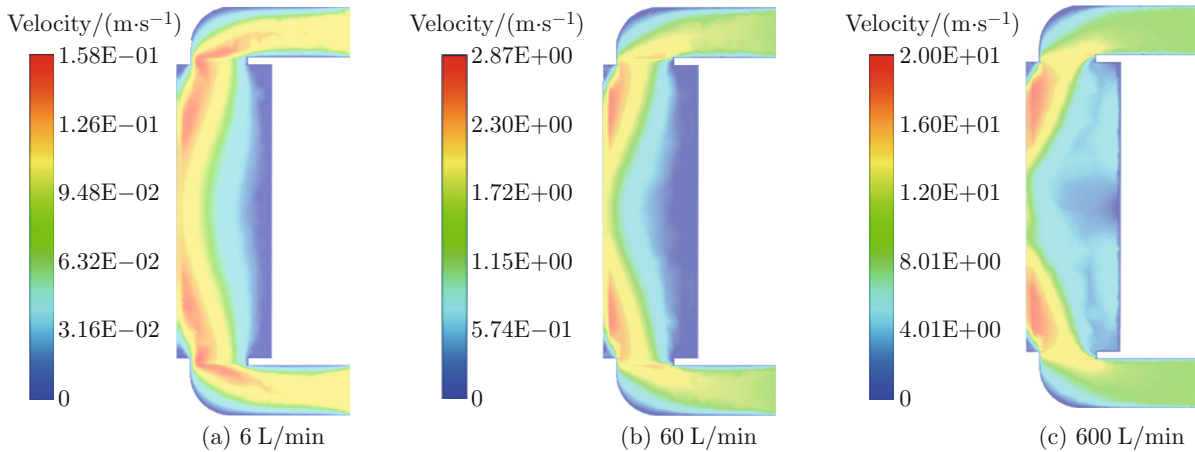


Fig. 9 Velocity distribution in inspiratory state

found that the air velocity in the outer guide channel is relatively uniform. When it enters the central part, due to the cross-sectional area's change, the velocity value rises, and the airflow accelerates through the two filter layers and then is inspired again. In the daily breathing state, when the respiratory rate is 60 L/min,

the pressure difference between the two sides is about 6.8 Pa, and the peak velocity is 2.87 m/s, which does not affect normal breathing. In extreme cases, when the respiratory rate increases to 600 L/min, the pressure difference reaches 250.3 Pa, and the peak velocity reaches 20 m/s.

When the state changes, the structure changes also. So, we get a new mesh. Then, we reset the inlet and outlet. Similarly, the expiratory velocity is set to 6 L/min, 60 L/min, and 600 L/min, separately.

According to the pressure distribution in Figs. 10 and 11, the average pressure of the central channel is higher than that of the outer channel in the expiratory state, and there is a slight pressure transition part at the filtering position; hence the filtration is completed under the radial gentle pressure difference. The velocity distribution shows that the central channel's gas has enough space for buffering; therefore, the

velocity distribution layer is uniformly formed. The velocity decreases after the expiration outlet. When the gas enters the outer channel, it is driven by the pressure difference; after that, speed is increased until it flows out. In the daily breathing state, when the respiratory rate is 60 L/min, the pressure difference between the two sides is about 16.7 Pa, and the peak velocity is 3.61 m/s, which does not affect normal breathing. Under extreme conditions, when the respiratory rate increases to 600 L/min, the pressure difference reaches 356.6 Pa, and the peak velocity reaches 25.9 m/s.

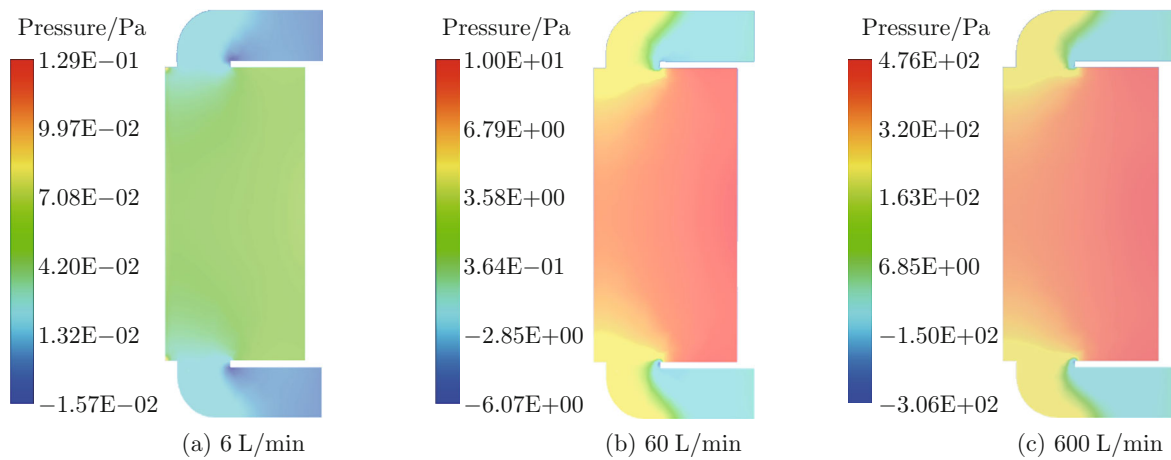


Fig. 10 Pressure distribution in expiratory state

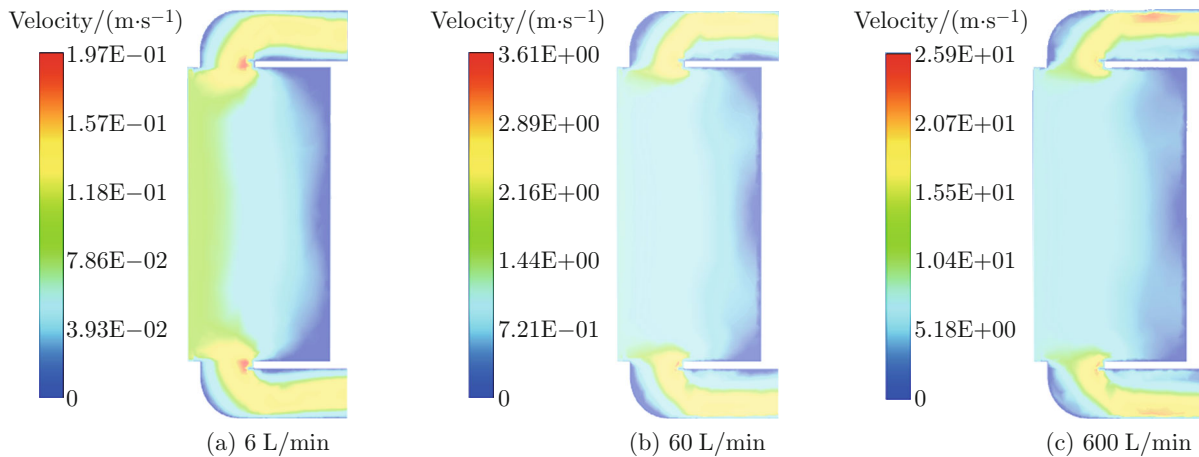


Fig. 11 Velocity distribution in expiratory state

3.3.3 Analysis of Results

Figure 12 shows the trend of peak pressure changing with respiratory rate, and it can be found that there are linear correlations between them. The expiratory resistance is slightly less than the inspiratory resistance, which is consistent with the design goal. The Chinese national standard YY 0469—2011 requires that

the inspiratory resistance does not exceed 49 Pa under an airflow rate of (85 ± 2) L/min. This airflow corresponds to a flow rate of about 1.5 m/s. At this air velocity, the pressure drop is about 10 Pa. Therefore, under the same airflow condition, our designed structure's resistance meets the standard's requirements, and the performance is improved. Although some ideal

assumptions are made in the simulation process, the results show that the proposed mask structure is feasible and reliable. It can meet the bidirectional filtration and low respiratory resistance requirements.

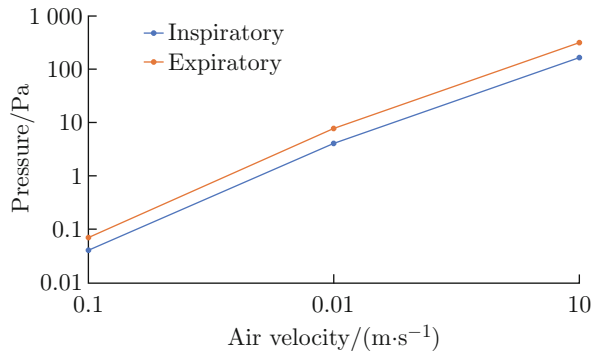


Fig. 12 Distribution of pressure peak with inlet velocity

4 Performance Test

4.1 Mask Making

The existing masks on the market are sampled to test and verify the practicability of the designed masks. The materials used are the medical-surgical mask, melt-blown cloth, non-woven fabric, sealing machine, self-designed and 3D printing parts.

Initially, the cloth is cut as the purposed design, and the sealing machine fixes the boundary to ensure the consistency of the shape. After that, the cut cloth is fixed on the replaceable filter material carrier. Finally, all parts are assembled on the existing mask, and the mask is made. The demo of the mask is shown in Fig. 13.



Fig. 13 Front and back of mask sample

4.2 Wearing Experience

In overall evaluation, the total mass is 15 g, similar to the standard N95 masks. First, comfort and airtightness were monitored, according to the standard of GB/T 2428—1998. Ten male and female subjects were required to wear a facial mask. Check before the test, including no movement trend of the mask, not too loose

or tight of the mask belt, the nose clip suitable for the nose bridge, and no air leakage around.

The subjects were asked to do the following six actions, each for 1 min.

(1) Normal breathing: standing position; average breathing speed; no speaking.

(2) Deep breathing: standing position; slowly and deeply breathing; pay attention not to over expire.

(3) Turn your head left and right: standing position, turn your head slowly to one side, and then turn to the other side after reaching the limit position. The breathing should be taken for each extreme position.

(4) Move your head up and down: slowly lower and raise the head. Inspiration should be taken at a limited position during the head-up movement.

(5) Speaking: speak slowly and loudly and ask subjects to count down from 100 or read a passage.

(6) Normal breathing: same as (1).

After the above steps of the test, the selected subjects scored the user experience, with a score range of 0—5, and the final average score was 4.2 points.

4.3 Organization Inspection

The final mask’s prototype is sent to the Institute of Fiber Inspection of Shanghai Institute of Quality Inspection and Technical Research for inspection and test. The main aims are to test the ventilation resistance and bacterial filtration efficiency. According to the standard YY 0469—2011, the test results are shown in Table 3.

Table 3 Detection result

Test item	State	Test value	Standard value
Ventilation resistance	Inspiration	34.0 Pa	49.0 Pa
	Expiration	24.0 Pa	29.4 Pa
Bacterial filtration efficiency	Inspiration	92.6%	95%
	Expiration	86.4%	95%

As shown in Table 3, the mask’s bacterial filtration efficiency is 92.6% on the front side and 86.4% on the backside, which does not meet the standard. However, the filtration performance of the original mask may be affected by the assembly process. The positive ventilation resistance of the mask is 34 Pa, and the negative ventilation resistance is 24 Pa. The front face corresponds to inspiratory, and the reverse corresponds to expiration. Compared with the 49 Pa in the standard, the mask meets the standard’s requirements, and its performance is improved.

5 Conclusion

This paper developed a bi-directional filtering mask with low resistance, which has the advantages of small structure change, easy access to materials, lightweight, and can be applied to masks’ daily use. The simulation

results show that the expiratory resistance is 35.66 Pa, and inspiratory resistance is 25.03 Pa at a flow rate of 60 L/min. The simulation results show that the designed structure's respiratory resistance is 72.7% and 51.1% of the standard, separately, which meets the standard's requirements in the normal breathing state. At the same time, the expiratory resistance is 70% of the inspiratory resistance. The expiratory resistance is reduced under the same condition, hence a more comfortable feeling during breathing. Under the safety condition of two-way filtration, the expiratory resistance is reduced, and the overall comfort is effectively improved. The simulation results are verified by mechanism detection.

Moreover, the sample can be reused for replacement. This structure can be disassembled and applied to different masks to improve respiratory resistance. The structure can be repeatedly disinfected by ultraviolet light.

Acknowledgment We thank Renaldy Dwi Nugraha for proofreading and the Base for Interdisciplinary Innovative Talent Training.

References

- [1] LI Q, GUAN X H, WU P, et al. Early transmission dynamics in Wuhan, China, of novel coronavirus-infected pneumonia [J]. *The New England Journal of Medicine*, 2020, **382**(13): 1199-1207.
- [2] LEUNG N H L, CHU D K W, SHIU E Y C, et al. Respiratory virus shedding in exhaled breath and efficacy of face masks [J]. *Nature Medicine*, 2020, **26**(5): 676-680.
- [3] RUBIO-ROMERO J C, PARDO-FERREIRA M D C, TORRECILLA-GARCÍA J A, et al. Disposable masks: Disinfection and sterilization for reuse, and non-certified manufacturing, in the face of shortages during the COVID-19 pandemic [J]. *Safety Science*, 2020, **129**: 104830.
- [4] FENG S, SHEN C, XIA N, et al. Rational use of face masks in the COVID-19 pandemic [J]. *The Lancet Respiratory Medicine*, 2020, **8**(5): 434-436.
- [5] BEESON S, BEHARY N, PERWUELZ A. Universal masking during COVID-19 pandemic: Can textile engineering help public health? Narrative review of the evidence [J]. *Preventive Medicine*, 2020, **139**: 106236.
- [6] ERICKSON M M, RICHARDSON E S, HERNANDEZ N M, et al. Helmet modification to PPE with 3D printing during the COVID-19 pandemic at duke university medical center: A novel technique [J]. *The Journal of Arthroplasty*, 2020, **35**(7): S23-S27.
- [7] WEBER C. Testing PPE: Are DIY masks a viable alternative to address shortages? [J]. *IEEE Pulse*, 2020, **11**(3): 29-30.
- [8] RODRIGUEZ-PALACIOS A, COMINELLI F, BASSON A R, et al. Textile masks and surface covers: A spray simulation method and a "universal droplet reduction model" against respiratory pandemics [J]. *Frontiers in Medicine*, 2020, **7**: 260.
- [9] O'DOWD K, NAIR K M, FOROUZANDEH P, et al. Face masks and respirators in the fight against the COVID-19 pandemic: A review of current materials, advances and future perspectives [J]. *Materials*, 2020, **13**(15): 3363.
- [10] SMITH P B, AGOSTINI G, MITCHELL J C. A scoping review of surgical masks and N95 filtering facepiece respirators: Learning from the past to guide the future of dentistry [J]. *Safety Science*, 2020, **131**: 104920.
- [11] ZUO S Y, CHEN Y H, ZENG C, et al. Application scope and relevant standards of masks in various countries [J]. *Chinese Journal of Infection Control*, 2020, **19**(2): 109-116 (in Chinese).
- [12] DING W B, JIA X D. Comprehensive assessment on protective performance of common self-inhalation filter type respirators [J]. *Journal of Environmental & Occupational Medicine*, 2018, **35**(5): 428-433 (in Chinese).
- [13] SHI G Y, GAO Q J. Research on the development of nanofiber membrane used for mask based on patent perspective [J]. *Materials Review*, 2020, **34**(Z1): 552-556 (in Chinese).
- [14] LIU C, HE B, KE Q F. Effect of aerosol flow rate on the filtration efficiency and respiratory resistance of air filtration materials [J]. *Shanghai Textile Science & Technology*, 2020, **48**(5): 11-13 (in Chinese).
- [15] TIAN Z X, KIM B Y, BAE M J. A study on Healthy Breathing Pattern when wearing a mask [J]. *International Journal of Engineering Research and Technology*, 2020, **13**(7): 1562.
- [16] YAO B G, WANG Y X, YE X Y, et al. Impact of structural features on dynamic breathing resistance of healthcare face mask [J]. *Science of the Total Environment*, 2019, **689**: 743-753.
- [17] ZHANG K. Design and research of a double valve anti-haze mask [J]. *Modern Industrial Economy and Informatization*, 2020, **10**(1): 31-32 (in Chinese).
- [18] GU J H, CHEN R Y, ZHANG J, et al. The development of the diver's respiratory resistance regulation device [J]. *Journal of Naval Medicine*, 2012, **33**(5): 328-329 (in Chinese).
- [19] ZHU L D, YU L T. Application of a new type of gas supply valve in positive pressure fire air respirators [J]. *Fire Technique and Products Information*, 2016(9): 58-59 (in Chinese).
- [20] NIU T F, XU H X, ZHOU Y S. Design improvement of regulating valve for underwater breathing apparatus [J]. *Chinese Hydraulics & Pneumatics*, 2016(1): 78-81 (in Chinese).
- [21] ZENG Y, ZHANG Z N. Environment-based design (EBD): A methodology for innovative and creative design [J]. *Journal of Shanghai Jiao Tong University*, 2019, **53**(7): 881-883 (in Chinese).
- [22] MAKINO K, SAWAGUCHI M, MIYATA N. Research on functional analysis useful for utilizing TRIZ [J]. *Procedia Engineering*, 2015, **131**: 1021-1030.